Trajectory Modelling for Autonomous Driving *

Investigating the Artificial Potential Field Method-

Andreas Zieglmeir [1)] Toshiya Hirose[1)]
Stefan-Alexander Schneider[2)]

Although the focus of autonomous driving is on maximizing safety and efficiency, comfort and familiarity will play a key role in the adoption of autonomous driving. Therefore, it is important to develop algorithms that can mimic human driving skills and adapt to individual driving styles.

The potential field method (PFM) is an obstacle avoidance algorithm for autonomous driving that uses a repulsive potential field, as a environment model, to navigate the vehicle to the lowest risk potential. In this paper, the PFM is used in a overtake scenario at high speed, to test the impact of using prediction when calculating the ideal yaw rate. Analysis is done on how the potential field can be used for lane keeping while following a car and then for overtaking it.

A driving simulator is used to record human driving data and compare it with automated driving using a PFM as is proposed by [3], with modifications to enable future prediction.

KEY WORDS: **safety, driving simulator, risk curve,** lateral control, potential field, repulsive field, hazard map, autonomous driving, driver model

1. Introduction

The potential field method (PFM) is a collision avoidance algorithm, that was first introduced in robotics. The risk potential is an artificial measure of the danger of collision at any location. It was adapted for autonomous driving, to model the risk of collision with traffic participants, obstacles and road boundaries. The repulsive potential field can then be used to navigate the vehicle to the lowest risk potential, analogous to charged particles in an electromagnetic field [1]. This approach is intended to produce results, that are similar to human driving behaviour, while still providing the transparency of a whitebox model at a low computational effort.

Where approaches to the potential field method differ, is in the mathematical basis for the potential functions, aswell as in the way vehicle control inputs are determined. The algorithm used in this paper isbased on the “intelligent driving system for safer automobiles”, proposed by [3] , with exception to the changes mentioned.

We propose a temporal analysis, to distinguish the perception of moving and stationary hazard sources. This should improve the behaviour in situations, where high speed will increase the difference in the current location of hazard sources as compared to future positions. When two cars are driving alongside each other, the static approach to the potential field, could lead to that vehicle being overlooked, because the risk is only evaluated in front of the ego car.

2. Lateral Control Algorithm

The potential field U_{risk} is the sum of individual functions that model the repulsive potential of hazard sources (Eq. 2).

Risk potential for road and vehicles use equations 3 and 4 respectively.

$$J(\gamma_p) = \frac{1}{N_t}\sum_{i=0}^{N_t} U_{risk}\big(X(\gamma_p,t_i),Y(\gamma_p,t_i),\,t_i\big) * w_J(t_i) + q\gamma_p^2 \tag{1}$$

To determine the ideal steering behaviour, a set of yaw rate candidates is evaluated based on average risk potential on the ego vehicles resulting trajectory using J (Eq. 1). The term $q\gamma_p^2$ is a penalty for exaggerated steering and t_i is the future time, at which the ego vehicles position is being evaluated (Eq. 1). Compared to [2] an additional weight function $w_J(t_i)$ is added, to reduce the impact of risk potential: contributions that are further in the future, should be considered less.

2.1. Dynamic Potential Field

Especially for overtaking at high speed, there might be a benefit to predicting the obstacle vehicles position and not only the ego position when evaluating the repulsive field.

Using time-dependent ground truth information, equation 1 can be calculated based on the ideal prediction. U_{risk} at each point along the trajectory is calculated with the future obstacle states corresponding to the time the ego vehicle has to travel to reach that position (Eq. 2).

This way, we can study the influence of time dependent risk potential, that takes the evolution of the scenario and all actors into account.

We therefore introduce a time dependent potential field evaluation with eqation 2, where the risk potential of all moving obstacles N_v is evaluated to their predicted position at the prediction time t_{pred}. The road including all lanes N_l is not time dependent.

$$U_{risk}(X,Y,t_{pred}) = \sum_{i=0}^{N_l} U_{ri}(X,Y) + \sum_{i=0}^{N_v} U_{oi}(X,Y,t_{pred}) \tag{2}$$

$$U_r(X,Y) = w_r * \exp\left\{-\frac{(Y-Y_{rc})^2}{\sigma_r^2}\right\} \tag{3}$$

$$U_o(X,Y,t_{pred}) = \begin{cases} w_o * \exp\left\{-\frac{\big(X-X_{or}(t_{pred})\big)^2}{\sigma_{orX}^2} - \frac{\big(Y-Y_o(t_{pred})\big)^2}{\sigma_{oY}^2}\right\} & \big(X \le X_{or}(t_{pred})\big) \\ w_o * \exp\left\{-\frac{\big(Y-Y_o(t_{pred})\big)^2}{\sigma_{oY}^2}\right\} & \big(X_{or}(t) < X < X_{of}(t_{pred})\big) \\ w_o * \exp\left\{-\frac{\big(X-X_{of}(t_{pred})\big)^2}{\sigma_{ofX}^2} - \frac{\big(Y-Y_o(t_{pred})\big)^2}{\sigma_{oY}^2}\right\} & \big(X \ge X_{of}(t_{pred})\big) \end{cases} \tag{4}$$

Note that if $t_{pred} = 0$, we obtain the original equation as proposed by [2], an additional modification is to introduce a different variance in x direction for the front and rear sections of the obstacle σ_{ofX}^2 and σ_{orX}^2 in an effort to better model the human behavior.

*Presented at the JSAE Kanto International Conference of Automotive Technology for Young Engineers on March 7, 2024

1) Shibaura Institute of Technology, 3-7-5 Toyosu, Koto-ku, Tokyo 135-8548, Japan (E-mail: z523138@shibaura-it.ac.jp)
2) Kempten University of Applied Sciences, Bahnhofstraße 61, 87435 Kempten, Germany

2.2. Longitudinal Control

Early versions of the algorithm also use the slope of the potential field to determine acceleration [1]. With this approach, the same environment model can be used for both longitudinal and lateral control.

However, reducing the overall risk does not always lead to the ideal behavior. For example, when overtaking, closing the distance to the leading vehicle will cause a short term increase in risk potential. This has been solved by [4] using a separate algorithm to calculate a desired speed profile independent of the potential field.

We have found that using a regular Adaptive Cruise Control (ACC) system for longitudinal control in combination with the lateral control of the PFM comes very close to the desired behavior for overtaking and following. The use of an ACC system could allow the direct implementation of traffic rules and objectives [5].

The potential field could still be used to suggest a reduced speed if the overall risk potential ahead of the ego car is high, or to indicate whether overtaking is possible, but it does not directly affect the speed of the vehicle or the decision making process.

3. Experiment in Simulation

The scenario used to determine the ideal parameters of the algorithm is a single overtake scenario. This scenario consists of an infinite straight road with one travel lane and one passing lane. Each lane is represented by Equation 3 with separate weights for each lane type. The lead vehicle is placed in front of the ego vehicle in the travel lane (Fig. 1). The lead vehicle is modeled by equation 4.

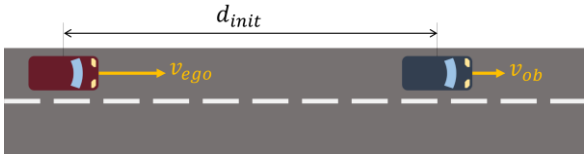

Fig. 1 Scenario for Training the model

3.1. Maneuver

The maximum speed of 100 km/h was chosen to ensure that the effect of prediction is noticeable in the results. As the difference between the two methods is expected to decrease at lower speeds, they will be equal when the hazards are stationary.

The ego car will start at the maximum allowed speed, 100 m behind the lead cars, each at 80 km/h. The ego car will then follow the first car until the driver has approached his preferred distance.

The scenario is run on a D3sim (Mitsubishi Presicion Company, Limited) powered driving simulator at Shibaura Institute of Technology to record human data for training and comparison. The simulation data is then converted to Open Simulation Interface (OSI)-compatible data, which is resimulated on Kehrmaker2, an OSI-based simulator developed at the University of Applied Sciences Kempten. Note that while the D3sim has a physics model for vehicle dynamics, the algorithm run on the OSI sim converts the requested yaw rate candidate γ_p directly into a circular trajectory.

4. Results

Human driving data was collected for both the following and overtaking portions of the scenario. In the following analysis, only data points starting 6 seconds before the overtaking request were used. A total of 10 runs were recorded, performed by one test subject, of which one was considered an outlier and was therefore removed (Fig. 2).

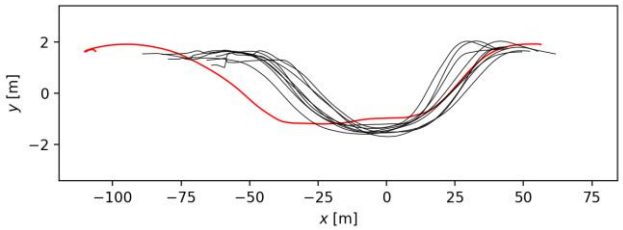

Fig. 2: Recorded human trajectories relative to obstacle position. Outlier is highlighted in red.

Using the regression procedure proposed in [3] but adapted to the new parameters. The parameters of the lead vehicle w_o, σ^2_{orX}, σ^2_{ofX} and σ^2_{oY}, where fitted, setting the road parameters to estimated values:

$$\begin{bmatrix} w_o \\ \sigma^2_{ofX} \\ \sigma^2_{orX} \\ \sigma^2_{oY} \end{bmatrix}_{opt} = \underset{w_o,\sigma^2_{ofX},\sigma^2_{orX},\sigma^2_{oY}}{\arg\min} \sum_{i=0}^{N_p} \left(\frac{\partial}{\partial Y} U_{risk}(\Delta X_i, \Delta Y_i, 0) \right)^2 \quad \text{subject to} \quad \begin{bmatrix} w_{rt} \\ \sigma^2_{rt} \\ w_{rp} \\ \sigma^2_{rp} \end{bmatrix} = const \tag{5}$$

Then the parameters of the travel lane w_{rt} and σ^2_{rt} and the passing lane w_{rp} and σ^2_{rp} are fitted using Equation 6:

$$\begin{bmatrix} w_{rt} \\ \sigma^2_{rt} \\ w_{rp} \\ \sigma^2_{rp} \end{bmatrix}_{opt} = \underset{w_{rt},\sigma^2_{rt},w_{rp},\sigma^2_{rp}}{\arg\min} \sum_{i=0}^{N_p} \left(\frac{\partial}{\partial Y} U_{risk}(\Delta X_i, \Delta Y_i, 0) \right)^2 \quad \text{subject to} \quad \begin{bmatrix} w_o \\ \sigma^2_{ofX} \\ \sigma^2_{orX} \\ \sigma^2_{oY} \end{bmatrix} = \begin{bmatrix} w_o \\ \sigma^2_{ofX} \\ \sigma^2_{orX} \\ \sigma^2_{oY} \end{bmatrix}_{opt} \tag{6}$$

Since the squared slope of the potential field in the y-direction is used as the cost function in Equation 6, the y-variances will tend to infinity. To keep the values in check, the variance of the travel lane is chosen so that twice the standard deviation is equal to the path width. This constrains σ^2_{rt} to 2.4 during optimization.

A Non-Linear Least Squares method was used for the regression task. To avoid the computational burden of running the simulation for each evaluation of the cost function, the relative position of the ego vehicle to the hazard sources was calculated in a single simulation run for each recorded human trajectory. Training was performed using the relative position data on a static image of the potential field. This results in the potential field shown in Figure 3, with values listed in Table 1.

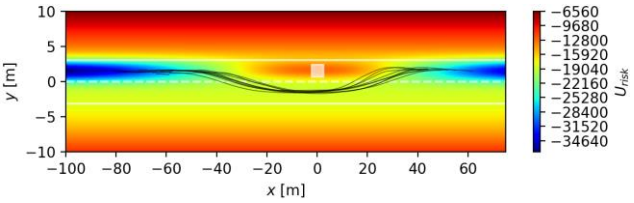

Fig. 3: From the perspective of the obstacle: trajectories used for training (black trajectories) and the resulting repulsive field.

Table 1 PFM parameters

Symbol	Value
w_o	26606
σ^2_{ofX}	3190
σ^2_{orX}	3864
σ^2_{oY}	2.06
w_{rt}	-22236
σ^2_{rt}	2.4
w_{rp}	-18430
σ^2_{rp}	130

During initial testing of the training script, the difference in risk potential to the left and right of the lead vehicle seemed to be quite small, which sometimes led to overtaking to the left of

the vehicle in non-ideal situations. The probable reason for this is that the human driver kept to the left of the center of the lane during lane keeping. This caused the optimization to reduce the weight of the passing lane. A solution to this problem could be a skew term in the equation of the lane potential field, or a different approach to training, this is left for future work. To avoid this issue for the scope of this paper, the driver was instructed to stay in the center of the lane when recording the data for this paper.

4.1. Algorithm Evaluation

The automated trajectory was recorded using the lateral control algorithm described in sections 2.1 and 2.3. The speed recorded in D3sim was used as the open loop speed input. Automation was performed using static analysis with $t_{pred} = 0$ and predictive risk (equation 4). For equation 1 J was calculated to future time t_{max} =1s, q=200 and the weight function is constant $w_J(t_i)$=1. The potential field of the passing lane is initially disabled and gets activated at the same time, the human driver was instructed to initiate the overtake.

Table 2 Resulting MAE values

Run #	Static [m]	Predictive [m]
1	0.880	0.348
2	0.595	0.351
3	0.777	0.217
4	0.643	0.309
5	0.707	0.275
6	0.407	0.379
7	0.437	0.243
8	0.505	0.269
9	0.369	0.306
Avg.	0.591	0.299

The automated trajectory is evaluated by the mean absolute error (MAE) to the human trajectory. The results are shown in Table 2. The results were consistently improved in each run by using prediction. The average MAE for the static risk trajectory over all nine runs is 0.591 meters. The same metric for predictive risk is 0.299. This shows that the ability to model human behavior can be improved by implementing a predictive performance method. Prediction generally shows an improved ability to navigate to a lower risk potential. On average, it is only 9 cm away from the lowest risk position, compared to 54 cm without prediction.

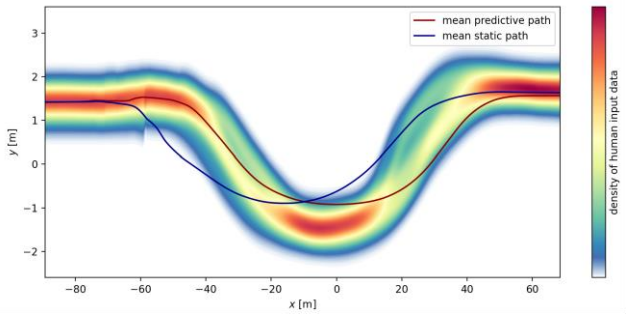

Fig. 4: Mean of the trajectories of both static(blue) and predictive (purple) PFM on top of the distribution of the human trajectories.

Figure 4 shows the resulting path taken by both iterations. While the predictive algorithm is much closer to human driving than the static algorithm, there are still visible differences in how much of the passing lane is used and how quickly the ego vehicle returns to the lane.

5. Conclusion

In this paper, a predictive evaluation for the potential field method has been implemented and analyzed. When predicting the future ego position to sample the potential field, the future position of the obstacles is used for the potential field function. In the simulation, this was achieved by using the available ground truth knowledge of the position of the obstacles at any point in time, providing a perfect prediction.

The method was trained on and compared to a set of human trajectories, of a single test subject. When the lateral control algorithm was compared to human behavior, the prediction provided better results, showing a large potential gain in using a predictive method. But the experiment needs to be repeated with different drivers to confirm the results.

It should be noted that the prediction method used cannot be applied in real life, and the improvement provided by prediction is expected to decrease at lower speeds. Nevertheless, the results still show a promising potential for using prediction to significantly improve the performance of PFMs (ignoring the computational cost).

An additional simulation was performed on a double overtaking scenario, inspired by the "Einscherer" scenario, to test the impact of overlapping risk potential and whether it is possible to re-enter the lane between two cars before overtaking again. However, with the chosen parameters, full re-entry was only possible at a distance of about 120 m between the two obstacle cars when using predictive risk. This suggests that the field parameters used in this paper are not robust enough to successfully navigate a wide range of situations.

The initial finding that the algorithm is able to accurately navigate to the lowest risk, but that the lowest risk does not correspond to human behavior, suggests that large improvements are possible in the potential field itself. Future work will determine whether this is a limitation of the potential field functions, the training data, or the training method.

Future work also includes the development of longitudinal control to best match the driver's behavior when following the lead vehicle. While following the lead vehicle, the risk potential parameters of the potential field are set to different values to prevent the vehicle from leaving the lane. The goal is to switch the weights of the hazard sources once the decision to overtake has been made.

References

(1) D. Reichart, J. Shick : Collision avoidance in dynamic environments applied to autonomous vehicle guidance on the motorway, IEEE Xplore, Intelligent Vehicles ’94 Symposium, Proceedings, (1994) p. 1, 3.

(2) P. Raksincharoensak, T. Hasegawa, M. Nagai : Motion Planning and Control of Autonomous Driving Intelligence System Based on Risk Potential Optimization Framework, AVEC’14, (2015) p.54 - 56.

(3) H. Inoue, P.Raksincharoensak, S. Inoue : Intelligent Driving System for Safer Automobiles, Journal of Information Processing, (2017)

(4) W. Sukittipattanakul, H. Inoue, K. Uehara : Autonomous Driving System using Speed Profile and Risk Potential Optimization based on Curviliniear Coordinate p. 4

(5) H. Winner, S. Hakuli, F. Lotz, C. Singer : Handbuch der Fahrerassistenzsysteme, Springer Vieweg, Third Issue (2015), p. 854 f.